

## Radars Astronomy

Rotation rates of Venus and Mercury and density of the atmosphere of Mars are recent radar discoveries.

Von R. Eshleman

Radars astronomy has sometimes been described in terms of the ways in which it differs from passive radio astronomy. In particular, it differs in that it uses man-made radiations to illuminate the target, so that the echoes reflected by the target may be studied; in passive radio astronomy it is the natural emissions from astronomical sources that are studied. Radars astronomy might also be compared with space science. In conducting research in these two areas, man reaches into space with measuring probes (electromagnetic in one case and material in the other) which are of his making and hence under his control. In some of the experiments I discuss here, such as measurement of the atmosphere of Mars during the Mariner IV flyby, the reach into space is made with a combination of a space vehicle and electromagnetic radiation.

Initial characteristics of a radar probe, such as its center frequency, time of start, polarization, and delay and frequency spectra, can be known and controlled with precision. When the echo is received, after interaction with a distant target, it can be compared with the radiation that was transmitted, for detailed study of properties of the reflecting body and the intervening medium. From echo time-delay

and frequency, dispersion in the delay and frequency, and echo strength and polarization, radar astronomers have been gaining new information about (i) the size and shape of the solar system, (ii) lunar and planetary surfaces, (iii) planetary atmospheres, (iv) the rates of rotation of Venus and Mercury, (v) the dynamics and long-term changes of the solar corona, and (vi) the density and irregularities of the interplanetary medium.

My aim here is to describe very briefly fundamental principles of radar astronomy, to give highlights of recent research with earth-based transmitters and receivers (monostatic radar astronomy), and to describe initial results and future potential of radar investigations in which one terminal is on the earth and the other is on a space vehicle (bistatic radar astronomy). Several excellent review articles on monostatic radar studies of the moon and planets have been published recently (1), so my treatment of this area is shorter than the importance of the subject would generally dictate.

### The Developing Technology

In a sense, radar astronomy had its origin more than 40 years ago, long before the "invention" of radar for the detection of ships and planes, when a pulsed radio transmitter and a receiver were used to measure a celestial target,

our ionosphere (2). However, the birth date of radar astronomy is usually given as 1946, when echoes from the moon were first detected (3). While very great improvements in radar systems were made in the years following the first lunar radar contact, the next step out into space was not possible until 1959, when recordings were made of echoes from the sun (at Stanford University) and Venus (at the Massachusetts Institute of Technology's Lincoln Laboratory) (4, 5). In 1961, almost daily measurements of the sun were started at M.I.T.'s Texas field site, and more detailed studies of Venus were begun by groups at the NASA/JPL [Jet Propulsion Laboratory] tracking station in California; at the Lincoln Laboratory's Massachusetts field site; at the Radio Corporation of America's laboratories in New Jersey; at Jodrell Bank, England; and in the Crimea, U.S.S.R. (6).

The step from the moon to Venus and the sun was difficult because echo strength for a given monostatic radar system is proportional to  $\sigma (4\pi R^2)^{-2}$ , where  $R$  is the distance of the target from the radar site and  $\sigma$  is the target's radar cross section. The range factor is of overriding importance in monostatic radar astronomy, causing an echo from Venus, when the planet is nearest the earth, to be about  $10^7$  times weaker (weaker by 70 decibels) than an echo from the moon, even though Venus is larger. For a smooth, perfectly reflecting, spherical target,  $\sigma = \pi a^2$ , where  $a$  is the radius. Planetary radar cross sections differ from  $\pi a^2$  because surfaces are not smooth, because they are not perfectly reflecting, and possibly because there is atmospheric absorption. Cross sections for the terrestrial planets at decimeter wavelengths, when normalized by  $\pi a^2$ , are from one half to twice the normalized cross section for the moon,  $\sigma/\pi a^2 \approx 0.07$ .

In addition to the factors governed by the target and its range, echo strength is proportional to  $P_T G_T A_R$ , where  $P_T$  is transmitter power,  $G_T$  is the gain of the transmitting antenna, and  $A_R$  is the aperture (approximately

The author is professor of electrical engineering at Stanford University, Stanford, California, and co-director of the Stanford Center for Radar Astronomy.

the area) of the receiving antenna. Antenna gain and aperture are related as  $G\lambda^2 = 4\pi A$ , where  $\lambda$  is the radio wavelength. Echo strength must also be compared with noise energy, which is always present. At meter wavelengths, radar system noise increases rapidly with increasing wavelength, the noise being due to cosmic sources in the beam of the receiving antenna. At decimeter and centimeter wavelengths the limiting noise is usually generated in the receiver itself.

The detection of Venus by radar depended upon improvements in all of the factors that are under the control of the radar astronomer:  $P_T$ ,  $G_T$ ,  $A_R$ , and the receiver noise temperature. In addition, new techniques in data processing were of critical importance in summing weak echoes over extended periods of time in order to make definitive measurements. Continuing improvements in all these areas have increased radar sensitivity for planetary studies by a factor of about 10 every 2 years since radar astronomy began, in 1946; that is, there has been a total improvement of more than a factor of  $10^{10}$ , or 100 decibels. Antenna diameters now range up to 1000 feet (300 meters); average transmitter powers, to several hundred kilowatts; and system noise temperatures, to as low as  $15^\circ\text{K}$ . Venus and Mercury can now be tracked all the way around their orbits, and fairly detailed radar-reflectivity maps of the moon (resolution of a few kilometers) are now being obtained. Continuing improvements based on shortening the operating wavelength (to increase  $G_T$ ) and on increasing antenna size and transmitter power are feasible, though costly.

Unfortunately, developments in the radar study of the sun have not been so striking. There has been little improvement during the past 5 years in the long-wavelength radar systems needed for solar studies. Improved systems of this type would be useful not only for investigations of the sun but also for studies of other plasma targets in the solar system, such as planetary ionospheres and the interplanetary medium (7). They could also be used to complement planetary surface studies made at shorter wavelengths.

The severe limitation of the range factor in radar astronomy can be circumvented by carrying the radar transmitter and receiver on a spacecraft closer to the target. While this technique will surely find important appli-

cations in future deep-space missions, it tends to be limited by the generally stringent limitations on instrument size and weight, spacecraft power, antenna size, and rate of transmission of data, and by the possibility that the radar pulses will interfere with other spacecraft instruments.

In bistatic radar astronomy, since only one terminal of the radar system is carried on the spacecraft, the other being on the earth, a part of the improvement in the range factor mentioned above for spacecraft systems can be realized, without all the disadvantages. For example, if the spacecraft is the receiving terminal, only a small, lightweight receiver using little spacecraft power is needed, and use is made of the very great  $P_T$  and  $G_T$  capabilities of the terminal on the earth.

The bistatic mode has several additional features which make it of interest in astronomical investigations. It adds a new dimension for the study of planetary surface and subsurface characteristics. In monostatic radar, only the energy reflected and scattered directly back along the line of incidence can be received. In the bistatic geometry, all scattering directions can, in principle, be studied for each angle of incidence, so that the complete scattering function and its dependence on wave polarization are obtainable. Since a spacecraft near a planet could receive the direct wave from the earth as well as signals reflected from the planet, there are self-calibration possibilities for accurate determination of the delay and frequency spectrums of the echo, as compared with the characteristics of the incident wave. This feature may also provide an opportunity to make radar-reflectivity maps of the surface, in order to obtain a rather detailed look at the surface features of cloud-covered Venus, for example.

If the spacecraft is on a trajectory that carries it behind the planet as viewed from the earth, the direct and reflected waves merge at occultation, the direct wave being much the stronger. Just before occultation the direct wave would traverse the atmosphere of the planet. Mariner IV demonstrated that measurements of signal characteristics just before and just after occultation can provide very accurate data for study of fundamental properties of a planet's ionosphere and atmosphere.

Some have questioned my use of the word *radar* in describing experiments in which there is no discrete

reflecting target. However, *radar* is an acronym for radio detection and ranging, and a "target" which is distributed along the propagation path can be detected and studied through its effect upon the apparent range or distance between transmitter and receiver, as well as through its effect on other signal characteristics. Thus I suggest including under the heading "bistatic radar astronomy" not only experiments that involve surface reflections but also the following radio experiments made with one terminal on the earth and the other on a spacecraft: occultation studies of planetary atmospheres, occultation studies of the density and dynamics of the solar corona, propagation measurements of the interplanetary medium, and propagation studies of celestial mechanics and general relativity.

### Group and Phase Velocity

The special forte of radar is measurement of range and range rate (radial velocity) on the basis of echo time delay and Doppler frequency—that is, of group and phase velocity. Precision radar distance and velocity measurements have application to studies of celestial mechanics, relativity, the solar corona, the interplanetary medium and solar wind, and planetary atmospheres.

Prior to the use of radar in astronomy, optical measures of the angular positions of asteroids and planets, together with Newtonian laws of motion, had been used to determine the size and shape of the solar system. However, the astronomical unit, the mean distance between the earth and the sun, could not be determined as accurately as the relative distances between planets could be. That is, the shape of the solar system was better known than the size, and the astronomical unit could be specified with an accuracy no better than about 1 part in  $10^3$ .

With the first few radar measurements of Venus in 1961, the accuracy of the astronomical unit could be improved by several orders of magnitude. In fact, these measurements were so precise that they quickly showed up errors in the more accurate shape predictions. It was evident that the whole problem of the astronomical constants of the solar system should be reinvestigated.

A very intensive effort for this purpose is now under way at M.I.T.'s Lin-

coln Laboratory (8). With the radar data obtained since 1959, together with numerous optical observations, a 26-parameter fit is made to minimize residuals. These parameters include the astronomical unit and certain orbital characteristics, masses, and radii of the inner planets. It is now necessary to give the astronomical unit in light-seconds (499.004785) instead of in kilometers (149,598,000), since the accuracy of the radar measurement (1 part in  $10^8$ ) exceeds the precision of measurements of the velocity of light (1 part in  $10^6$ ). Improved data on planetary orbits, radii, masses, and densities have also been derived from this investigation (8).

With the precision that is now being obtained, it should be possible to provide a new test of Einstein's theory of general relativity in terms of the motion both of mass points and of electromagnetic radiation in an intense gravitational field (9). In fact, Ash, Shapiro, and Smith (8) report a somewhat better fit with general relativity than with Newtonian mechanics in the analysis that has been made to date.

Precision range-rate measurements have been used to track deep-space probes, and the data obtained have also been used to improve astronomical constants (10). In these investigations, as well as in the radar studies described above, it has been assumed that the waves propagate at  $c$ , the velocity of light. Because of the presence of free electrons along the path, however, the group velocity  $v_g$  (from which range is determined) is slightly less than  $c$ , while the phase velocity  $v_\phi$  (from which range rate is measured) is slightly greater—with  $v_\phi v_g = c^2$ . To the first order, the departures from  $c$  are proportional to  $N_e \lambda^2$ , where  $N_e$  is the average number density of electrons along the propagation path.

Relatively short radar wavelengths have usually been chosen to minimize the effects of the plasma. While it appears likely that plasma effects are not important in the deductions that have been made thus far, they will become important when a higher level of precision has been achieved, or for paths that encounter more electrons. Even shorter wavelengths will be used to reduce plasma effects still further, and attempts will be made to determine the extent of these effects by combining group and phase velocity measurements.

An alternative approach to this prob-

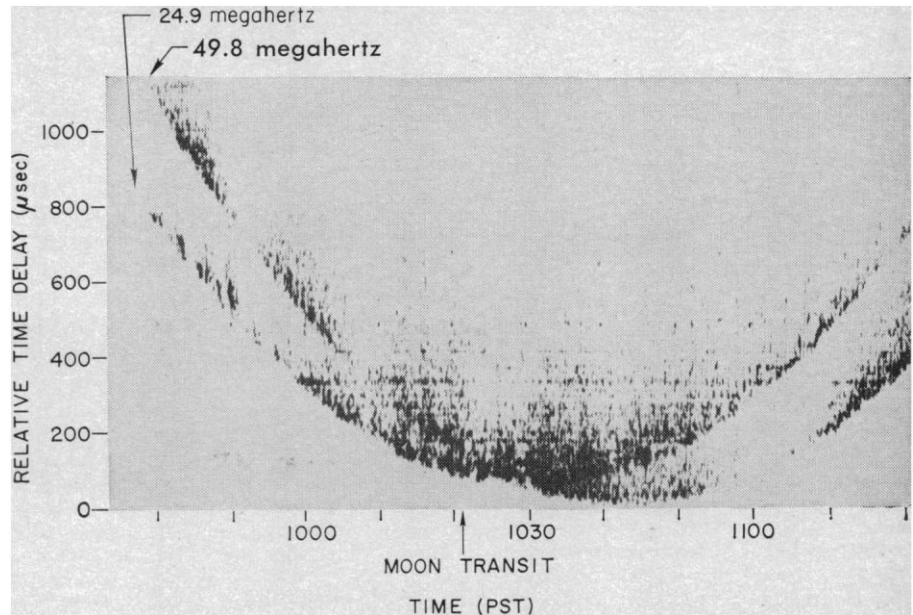


Fig. 1. Relative time delay of echoes from the moon at  $\lambda = 12$  meters (frequency, 24.9 megahertz) and  $\lambda = 6$  meters (49.8 megahertz). Differences in the position of the lower boundaries of the echoes are due to the presence of free electrons and to the changing range between the earth and the moon. These differences can be used to determine the amount of cislunar ionization.

lem is that of making measurements at two wavelengths simultaneously. Since it is known that the velocity perturbations are proportional to  $\lambda^2$ , the total ionization along the path and its changes with time can be measured from the differences in group and phase velocities at the two wavelengths. Thus, information about the ambient ionization in interplanetary space and near the sun and planets can be gained at the same time that correction terms for improving distance measurements are obtained.

This technique has been used at wavelengths of 12 and 6 meters to determine the ionization along paths between the earth and the moon (11). Figure 1 shows radar-echo indications at these two wavelengths as a function of time of day. The minima of the two curves would occur at the same ordinate and abscissa if earth-moon space were a vacuum. Conversely, the differences of the curves serve as a measure of the number of electrons in a column between the earth and the moon. The results are of interest in determining the amount, location, and variation of this cislunar ionization, and they could also be used to improve precision radar measurements of distances in the earth-moon system.

Two-wavelength measurements (at 6 meters and 0.71 meter) of the interplanetary density are being made with spacecraft of the new Pioneer series

(12). Radio transmissions from the earth are received in these interplanetary probes, where the signals are analyzed in terms of differential group and phase velocities. Measurements were made with Pioneer VI (the first of this series, launched on 16 December 1965) while it was within 0.6 astronomical unit of the earth and between 0.8 and 1.0 astronomical unit from the sun. Current measurements with Pioneer VII (launched 17 August 1966) are probing regions outside the orbit of the earth. The average number density of electrons in interplanetary space near the orbit of the earth has been found to be about 5 to 10 electrons per cubic centimeter, but on occasion the propagation paths are observed to become filled with streams of plasma of densities up to 60 electrons per cubic centimeter (12). An example is given in Fig. 2. Analyses of these data are not yet complete, but comparisons with local measurements of the solar wind at the spacecraft and near the earth lead us to expect that much more will be learned about the size, shape, motion, boundary characteristics, and density of these streams of solar plasma from active regions on the sun.

Propagation experiments of this type would be of special interest when the probe was on the far side of the sun. Radio signals could then be used for studying the density, structure, and dynamics of the inner and outer solar

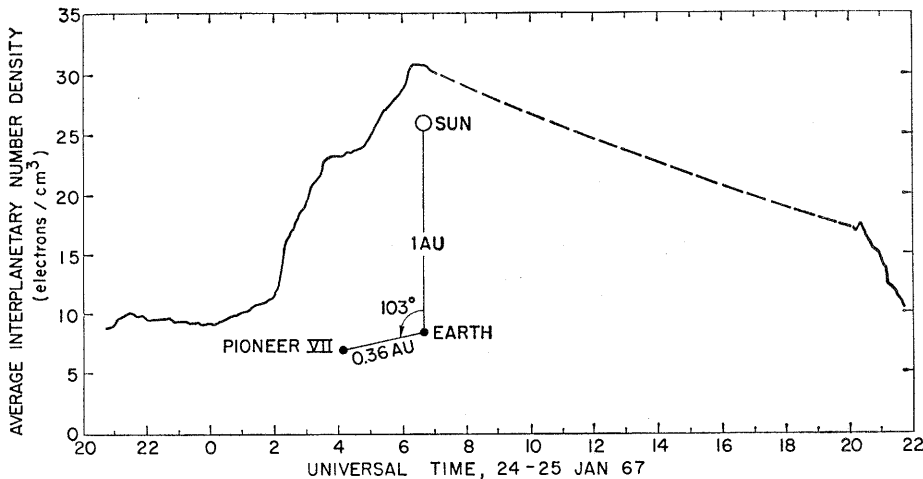


Fig. 2. Intrusion of a solar plasma stream into the path between the earth and Pioneer VII; the intrusion causes the average interplanetary number density along the path to change from about 10 to more than 30 electrons per cubic centimeter.

corona, from measures of phase and group velocity, wave polarization, and amplitude and frequency fluctuations. As the sun-earth-spacecraft angle decreased, the rays would go deeper into the corona, where eventually scattering, absorption, and bending would distort the signals beyond recognition. Radio astronomers track cosmic radio sources through this region to obtain information about the corona and, once the scattering effects are understood, a measure of the angular diameters of the sources (13). Mariner IV was tracked through this region even though only the low-gain antenna on the spacecraft was used (14). However, neither the cosmic radio sources nor the single short wavelength of Mariner IV can provide as much informa-

tion about the corona as would be available from stronger coherent signals at two or more wavelengths. It is expected that it will be possible to conduct such experiments with future Pioneer spacecraft, and a new series of spacecraft (Sunblazer) has been proposed primarily for making such coronal measurements. However, as discussed below, it might be advantageous to conduct these experiments in such a way that other measurements of scientific interest would be made at the same time.

Occultation of a spacecraft behind the solar corona would make possible accurate measurements of the general relativistic effect mentioned above. Figure 3 illustrates the separate effects of general relativity and an assumed uniform

spherical coronal density on the incremental path length (determined from a measurement in which  $v_g$  is assumed equal to  $c$ ) of a ray between the earth and a spacecraft about 1 astronomical unit from the sun. These effects are plotted as a function of the impact parameter (the distance from the center of the sun to the nearest point on the ray path), in solar radii. Note that the coronal plasma effect is dependent on wavelength. Range rate or phase velocity effects would be similar in kind, but the sign of the plasma contribution would be negative. While it may appear from Fig. 3 that the coronal effect could be made negligible by using a very short wavelength, it should be pointed out that the corona is highly variable in structure and density. Thus it may be important to use two or more wavelengths to measure the two effects (relativity and coronal plasma) so that they can be separated.

While Fig. 3 illustrates a predicted effect of the sun's gravity on electromagnetic waves, we need to know the "positions" of the terminal points in order to determine the extra apparent path length. But the motion of the end points is also affected by general relativistic considerations as well as by other forces. To avoid problems such as the need to determine the effects of radiation pressure and gas leaks on the average motion of the probe, we could "tie" the probe to a massive planet by placing it in an orbit around the planet. We could then also make use of all present knowledge about the orbit and position of the planet.

Thus the problems related to the solar corona, wave propagation in an intense gravity field, and the motion of planetary mass points in the gravity field could all be attacked together. This experiment would correspond to the radar experiment proposed by Shapiro (9), with the difference that the probe, acting as a radio transponder, would provide stronger and less disturbed signals than could be obtained by monostatic radar reflections from the planets themselves. In addition, the use of an orbiter would avoid problems associated with the unknown planetary radius and surface-reflection characteristics. Also, the use of two or more wavelengths would provide additional scientific information about the corona which could be used to refine the range and range-rate measurements needed to specify the relativistic effects with high precision.

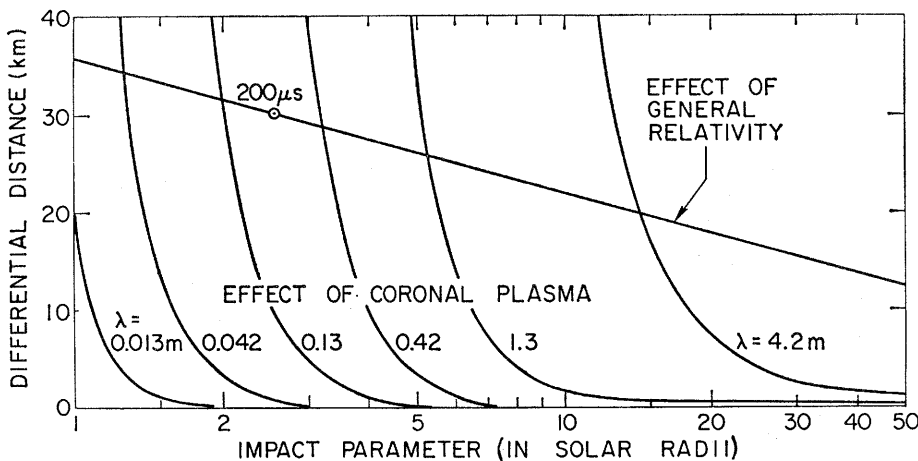


Fig. 3. Change in apparent radio path length between the earth and a probe at 1 astronomical unit from the sun, due to changes in group velocity caused by the solar corona and the general relativistic effect of the solar mass. The impact parameter is the distance from the center of the sun to the nearest point on the radio ray path. For a ray that passes the sun at 2.5 solar radii, a round-trip radio pulse is delayed an extra 200 microseconds by the relativistic effect.

## Delay and Frequency Spectra

Echo characteristics indicate properties of the radar target. Planetary radar echoes can be characterized in terms of total power, delay spectrum (echo power as a function of time delay), frequency spectrum (echo power as a function of Doppler frequency), and state of polarization. From these data, information can be derived on the electrical properties of the planetary crust and atmosphere, roughness parameters of the surface, planetary rotation, and axis orientation. The data can also be interpreted in terms of the scattering intensity as a function of position, to obtain a radar-reflectivity map of the planet.

Let us consider two kinds of transmitted radar pulses, one of such short duration that echo delay characteristics can be well defined, and one which is nearly monochromatic, so that echo-frequency characteristics can be specified accurately. A smooth planet would not spread the short pulse in time or the monochromatic pulse in frequency, but echoes from a rough, rotating sphere would exhibit spectral spreading in both time delay and Doppler frequency.

Figure 4 illustrates the delay spectrum for echoes from the moon at two wavelengths (0.036 and 0.68 meter) and at two polarizations for the longer wavelength (15). A number of important features of the moon are determinable from such measurements, and it is expected that, once direct study of the moon reveals physical surface and subsurface characteristics which can be compared with radar results, radar-echo studies of planets will take on added meaning.

Total echo energy for the polarized echoes from the moon does not change noticeably with radar wavelength from about 0.01 meter to 10 meters. (In Fig. 4, the values for polarized echoes have been normalized relative to the initial strong returns.) The measured cross section  $\sigma$  is about  $0.07 \pi a^2$ , a value which has been interpreted as indicating a relative dielectric constant of about 2.8 for the lunar crust (15). It is usually assumed that, in condensed form, the basic material of the lunar surface has a higher dielectric constant (above about 5), but that on the moon the material is loosely packed or porous. Even the value of 2.8 is higher than the value that has been derived from radiometric observations.

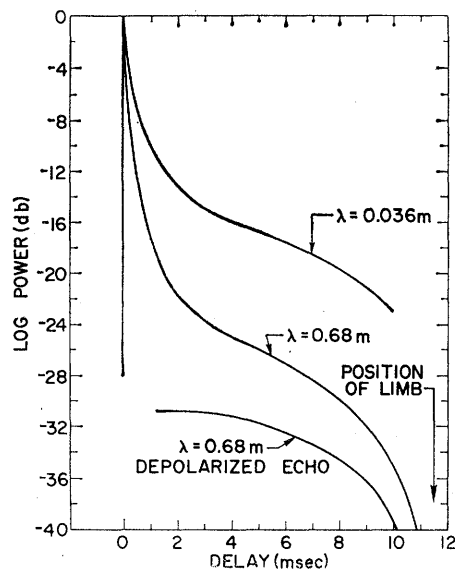


Fig. 4. Delay spectra (echo power measured as a function of time delay, normalized with respect to the leading edge of the moon) for polarized echoes from the moon at  $\lambda = 0.036$  and  $0.68$  meter, and a delay spectrum for depolarized lunar echoes at the longer wavelength. Pulse lengths of 30 and 400 microseconds were used for the measurement, respectively, of the polarized and depolarized echoes (15).

More recent radar studies by Hagfors *et al.* (16), based on detailed measures of linear polarization effects at various angles of incidence, may reconcile these results. They suggest a two-layer model having a tenuous top layer, a meter or two thick, with a dielectric constant of only 1.8, overlying a base layer having a dielectric constant of about 5. Additional evidence on this is available from the anomalously strong scattering from relatively new craters such as Tycho, which suggests that the top layer has been blown away, exposing a denser and hence more highly reflecting base layer (17).

For the first millisecond or so of relative delay (see Fig. 4), the lunar-echo energy decreases abruptly, the total change being greater at the longer wavelengths. This first part of the polarized echo is due to specular reflection of radiation reaching the gently rolling, relatively smooth lunar surface at normal incidence. Detailed study of this portion of the echo provides information on the average large-scale slopes, and the changes in delay spectra with change in wavelength show that average slopes are greater when measured over smaller distances.

For greater time delay, it appears that no large areas are tilted suffi-

ciently to give a specular echo, and the measured echo energy is due to scattering from wavelength-size, small-scale irregularities (rocks?) on or near the surface. This weak, diffuse component is stronger at the shorter wavelengths, an observation indicating an increase in small-scale "roughness" as the characteristic size being measured is made smaller. The depolarized component of scattering follows the general behavior of the diffuse polarized component, an observation which strengthens the belief that both components are due to small-scale irregularities.

Delay spectra and total-power measurements for the planets (1) indicate that Venus is more highly reflecting (by a factor of about 2) than the moon, and has less large-scale roughness, while producing comparable scattering due to wavelength-size, small-scale irregularities. Mercury appears to produce scattering more nearly like that from the moon, although Mercury seems to be somewhat rougher. Mars is harder to study because of its fast rotation and great range, but there appears to be a correlation of echo strength and visible surface features, with the dark areas scattering more strongly. Successful radar detection of Jupiter has been reported, but there are few quantitative details (18).

A very striking feature of the radar studies of Venus is the large reduction of  $\sigma$  at short wavelengths. At  $\lambda = 0.038$  meter, Evans *et al.* (19) report,  $\sigma$  is only about one-tenth the value obtained at  $\lambda = 0.12$  meter and longer. It appears that the energy is being returned from the surface, but the dense atmosphere may be causing attenuation, perhaps due to the presence of water vapor below the clouds. Added evidence on this matter may be obtained from the occultation experiments planned for the 1967 Mariner-Venus mission, on which three radar wavelengths (0.13 meter, 0.71 meter, and 6 meters) will be used to probe the atmosphere.

Figure 5 is an example of a radar-echo frequency spectrum for Venus (20). It shows echo power as a function of frequency relative to the Doppler frequency of the energy being returned from the specular point at the center of the disk. If the planet were not rotating relative to the observer, all of the echo energy would be returned at this center frequency. Because of relative motion, however, the

echo energy for a rotating planet is spread in frequency, with the hemisphere moving toward the radar causing positive Doppler shifts, and the other hemisphere giving echoes at frequencies lower than the central value. Study of such spectra gives information complementary to that obtained from the delay spectra concerning large- and small-scale features of the planetary surface, its electrical properties, anomalous scattering regions on the surface, and atmospheric effects. In addition, the combined spectra can be used for studying planetary rotation and for obtaining radar maps.

### Planetary Rotation

When the signal level in the frequency spectra is sufficiently high for accurate measurement of the Doppler-shifted energy from the limbs of a planet, it is obvious that the total frequency spread is related to the rotation period of the planet, its radius, and the orientation of its axis. By observing a planet of known radius over a period of some months, while the axis orientation relative to the observer changes, it is possible to separate and define uniquely the rotation period and the celestial latitude and longitude of the axis.

Scattering from planetary limbs is very weak as compared to that from the more central portions of the disk. The stronger echoes can be used to define rotation: echoes can be "processed" and thus made to give separate frequency spectra for different range "slices"—that is, for separate sections of the delay spectrum. In addition, if anomalous scattering centers stand out in the delay and frequency spectra, as illustrated in Fig. 5 for Venus, they may be tracked over a long period of time and used to define the rotation with precision, particularly if the same features can be identified in records taken over several years.

Early interest in this subject was centered on Venus, since no surface features can be seen on this cloud-covered planet and its rotation characteristics were unknown. Initial results indicated a long period of several hundred earth days, and there was a strong expectation that Venus might have a synchronous sidereal rotation period of 224.7 earth days. Thus it was suggested that Venus, like the moon and (as was thought) Mercury, might maintain the same hemisphere

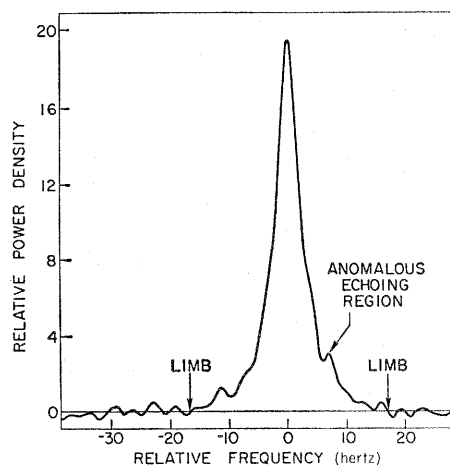


Fig. 5. Frequency spectrum (echo power measured as a function of relative Doppler frequency) of polarized echoes from Venus at  $\lambda = 0.125$  meter. The Doppler coordinates of the limb and an anomalously strong return from a small area on the surface are indicated (20).

toward its primary (for Venus, the sun) at all times (6, 21). Thus its rotation, while slow, would be direct (that is, counterclockwise as viewed from the north celestial pole), like the rotation of all the other planets except for Uranus, whose equator is inclined slightly more than 90 degrees from its orbital plane. However, more precise measurements soon showed that Venus rotated in the opposite, or retrograde, sense, with its equator near its orbital plane. It is thus quite unusual in its rotational characteristics as compared with its neighbors in the solar system.

In Fig. 6, measured values of the sidereal period of Venus are presented to show how the precision has increased with time (22). The value needed for synchronous (sun-locked) rotation is shown for comparison, and it is well away from the recently measured values in magnitude, as well as being wrong in sense.

The most recent studies give values near  $-243$  earth days for the sidereal rotation period of Venus, and Goldstein has suggested a value of  $-242.6 \pm 0.6$  days, from a study of the repeat of spectral features in 1964 and 1966 (22, 22a). As Carpenter has pointed out, these values are very close to a peculiar earth-lock condition at  $-243.16$  days (shown in Fig. 6), for which Venus would present the same hemisphere toward the earth at each inferior conjunction. (Adjacent other periods giving synodic commensurability are at  $-171.67$  and  $-416.68$  days.) It is not understood how such an earth-lock condition could be brought about,

since the forces involved are extremely weak (23). Yet the possibility of some connection with the earth takes on even greater speculative interest from the report that, to within about 1 degree, a value within the margin of error of the measurement, the rotation axis of Venus appears to be perpendicular to the orbit of the earth, while being about 3 degrees off normal relative to its own orbital plane (24). [One can hardly avoid mentioning, in this regard, the hypothesis put forth by Velikovsky (25), based on historical documents from many parts of the world but totally without justification on the basis of what we think we know about celestial mechanics, that Venus in historical times had a devastating close encounter with the earth.]

On a rather new chart in my office, the rotation period of Mercury is given as 87 days 23 hours 15 minutes 43 seconds. This quite precise value was obtained from the long-measured orbital period of Mercury and from a relatively few studies of faint visual markings on its surface. The results of these studies are consistent with synchronous (sun-locked) rotation of the planet such that the orbital period equals the sidereal rotation period.

One of the objectives of the early radar investigations of Mercury was that of testing, on a planet of "known" rotational period, the radar technique for determining rotation, to give credence to the results of the studies of the rotation of Venus. It was at first reported that such a check had been obtained, based on the width of weak-frequency spectra (26). However, Pettengill and Dyce used the more powerful technique based on separate frequency spectra for different parts of the delay spectrum, and found, to their considerable surprise, that the radar result was quite different from the expected 88 days. They obtained a value of  $59 \pm 5$  earth days, direct rotation (27). Reevaluation of the optical observations indicates that there are possible values other than the long-accepted value of 88 days, one being  $58.4 \pm 0.5$  days. In addition, theoretical studies show that a different sun-lock condition may well exist at two-thirds the orbital period, or 58.65 days, and the evidence that such is the case is now very strong (28).

The values given above for Venus and Mercury are sidereal periods. With reference to the sun, the length of the day on Venus is about 117 earth days, and on Mercury, about 176 earth days.

## Radar Mapping

The two dimensions (time delay and Doppler frequency) measured in echo spectra for a rough, rotating planet can be translated into radar scattering intensity as a function of position (latitude and longitude) on the planet. One can visualize this by noting that, on the planetary disk viewed from a monostatic radar site, echo energy at a particular delay or range is coming from a circular region centered at the disk's center, and echo energy at a particular Doppler frequency is coming from a strip parallel to the projection of the planet's spin axis on the disk. Common sources for a given delay and Doppler frequency are two small regions at the intersection of the delay or range annulus and the Doppler strip. Thus, such range-Doppler mapping has a twofold ambiguity, although this problem may be circumvented to some degree by use of narrow antenna beamwidths and of interferometric and data-processing techniques. The resolution is limited by system sensitivity: the smaller the resolution cell is, the smaller is its fraction of the total echo energy. Radar resolution can be better than the limit set in optical astronomy by ray bending in the earth's atmosphere, and radar has already surpassed optical resolution for regions near the limb of the moon (29).

Figure 7 represents the range-Doppler mapping technique at its current level of development. It shows (at left) a region near Copernicus as mapped at Lincoln Laboratory by an earth-based, monostatic radar and (at right) a photograph (also from the earth) of the same region (29). The grid lines are at 1-degree intervals (30 kilometers). The radar resolution is on the order of a few kilometers. As has been suggested, the illustrated radar resolution is about that of a Xerox reproduction of a good photograph of the moon taken from the earth.

Radar mapping is of special interest for Venus, since the cloud cover makes optical study impossible. A start has been made, even though, as mentioned above, monostatic echoes from Venus as obtained on the earth are weaker than lunar echoes by about 70 decibels. A number of regions which scatter more strongly than their surroundings do have been identified, and they may correspond to mountainous areas on Venus (22, 24).

Detection of surface features which are hidden from optical view by clouds

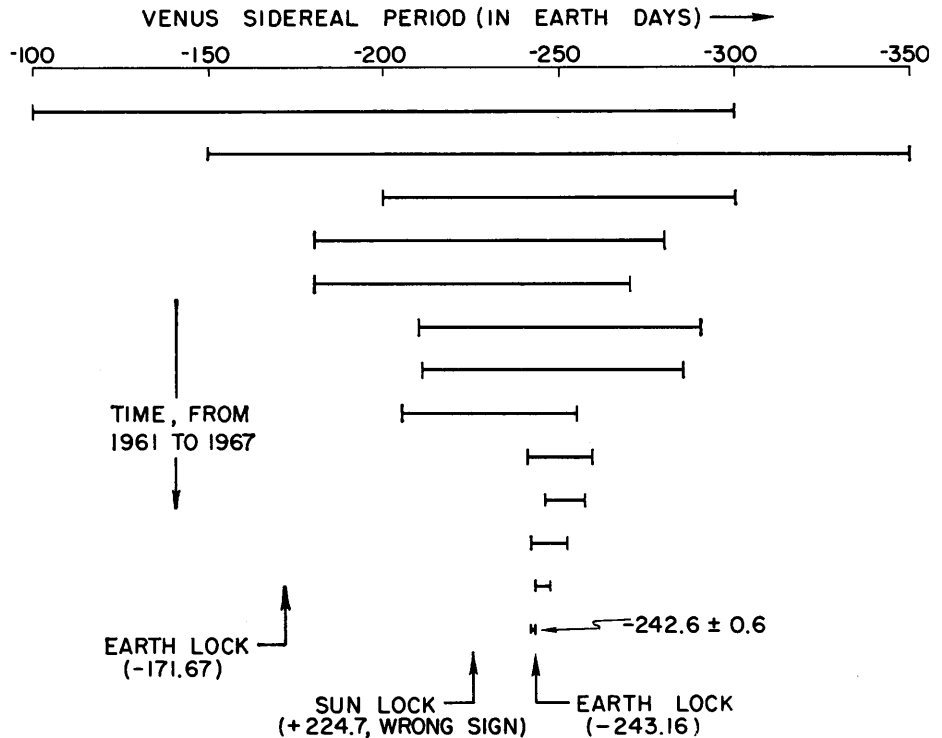


Fig. 6. Radar measurements of the sidereal rotation period of Venus, showing increase of precision with time and the current close agreement with a peculiar earth-lock condition in which the same hemisphere faces the earth at each inferior conjunction (22).

is not the only purpose of radar mapping. High-resolution radar at a number of wavelengths can probe beneath the surface and expose structure and materials on and near the surface which might not be resolved in remote optical study.

As noted above, the bistatic radar mode offers advantages for the study and mapping of planetary surfaces, in particular an increase in echo strength relative to earth-based measurements. A start toward demonstrating this potential has been made by receiving, on

earth, radio signals which were transmitted from a Lunar Orbiter spacecraft and reflected by the lunar surface (30). Here one obtains the two dimensions from just the frequency spectrum, by noting how it changes with time as the scattering geometry changes due to motion of the spacecraft relative to the scattering region and earth.

This technique is analogous to holography, where a coherent source of light is scattered from an object and a mixture of the scattered light and

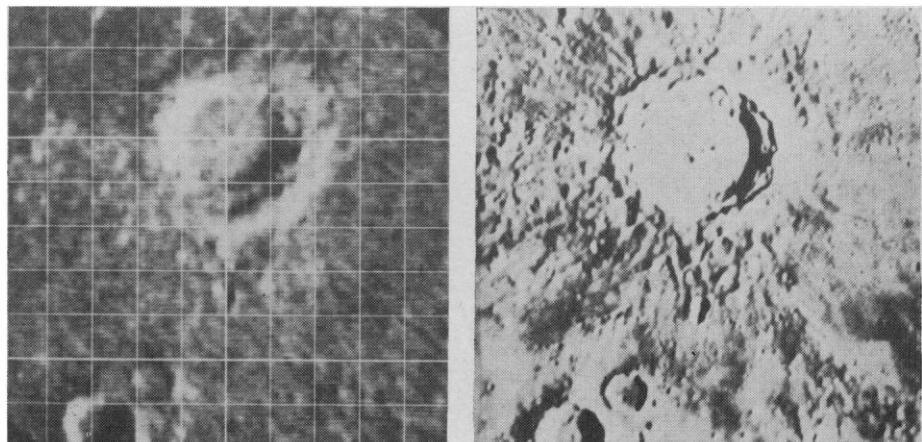


Fig. 7. (Left) Range-Doppler radar map of a region near Copernicus, made by the M.I.T. Lincoln Laboratory at  $\lambda = 0.038$  meter. The grid lines are at 1-degree (30-kilometer) intervals. [Courtesy G. H. Pettengill] (Right) Optical photograph of the same region. [Rectified Lunar Atlas (Univ. of Arizona Press, Tucson, 1963)]

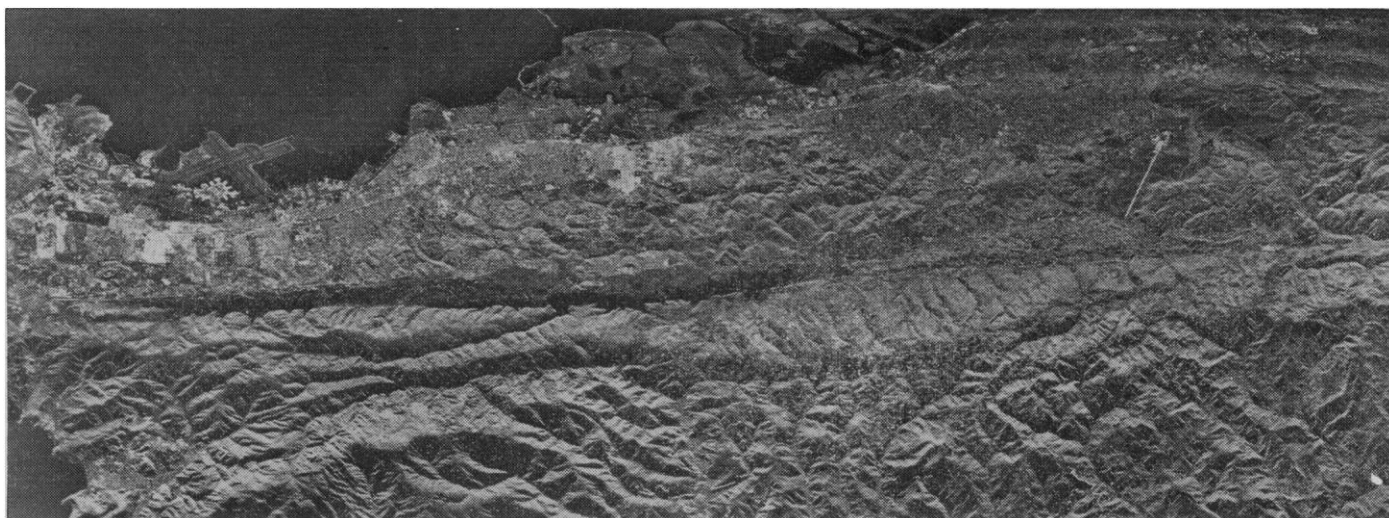


Fig. 8. Radar image of the San Francisco peninsula with the San Andreas fault zone across the center, the San Francisco Airport at left center, and Stanford's 2-mile linear electron accelerator at right center. [Courtesy U.S. Army Electronics Command and NASA]

the direct coherent light is recorded on film. After the film is developed, coherent light sent through the film produces a three-dimensional image of the object. For the radar hologram the coherent source is the radar transmitter and the object of study is the planetary surface. There is no direct comparison with the film, which picks up radiant energy on a two-dimensional surface. However, the spacecraft moving along in its trajectory near the planetary surface can receive a mixture of the direct and scattered energy, and this is equivalent to the exposure along a line on the film. But just as the two-dimensional film records information for a three-dimensional image, so the one-dimensional radar hologram contains information for a two-dimensional image of the scattering intensity as a function of position on the planetary surface—that is, a radar map.

The bistatic mode also makes it possible to study in detail the complete scattering characteristics of various surfaces as a function of angle of incidence and direction of scattering. Of particular interest is the very sensitive dependence of specular scattering near the Brewster angle on properties of the near-surface material, where one polarized component may not be reflected at all.

It is hoped that, in the near future, monostatic radars can be carried into orbit around other planets so that detailed radar maps can be obtained. The potential of this approach is well represented by the side-looking radar maps which are being taken, from aircraft, of regions on the earth, as illustrated in

Fig. 8. Features as small as a few meters can be resolved, and studies of the correspondence between the radar maps and characteristics of geological and agricultural interest could well have important application to all of the radar mapping techniques for planets (31). Until very large payloads and high power capacity are available on such spacecraft, however, it would seem that the bistatic mode has much to offer in that only a lightweight receiver and little power are needed on the spacecraft.

#### Solar Radar

Monostatic radar echoes from the sun (that is, from its highly ionized corona) have been obtained only at relatively long wavelengths. Near  $\lambda = 10$  meters, the sun is usually a good reflector and the radar cross section, while quite variable, can become many times greater than  $\pi a^2$ , the physical cross section. It appears that, at shorter meter-range wavelengths and at decimeter wavelengths, the radar energy is very strongly absorbed before it reaches the reflecting level, which becomes progressively deeper in the corona as the wavelength is shortened. Unfortunately, at the long wavelengths needed for solar radars, solar and cosmic noise, which tends to mask the echo, is very strong and  $G_T$  is relatively small for a given antenna size. Additional factors which make solar radar studies difficult include the wide Doppler bandwidth, depolarization of the echoes, and the nonthermal character of radio noise from the sun.

The original Stanford measurements were made at  $\lambda = 11.5$  meters, and a 40-kilowatt transmitter and a 28-acre (11-hectare) antenna were used (4). While the marginal echoes demonstrated the feasibility of radar studies of the sun, few quantitative results were obtained. James (32) has recently reported on the results of a 4-year study during which radar echoes from the sun were obtained on about 1000 days at M.I.T.'s El Campo, Texas, field site. A wavelength of 7.85 meters is being used in these measurements, the transmitter power is up to 500 kilowatts, and the antenna, which is more efficient per unit area than the Stanford antenna, covers about 9 acres.

Figure 9 illustrates the results for the radar cross section of the sun. The 3-month average value of  $\sigma$ , normalized with respect to the photospheric-disk size,  $\pi a^2$ , is plotted and compared with the yearly average number of sunspots. The most striking feature is the large decrease in cross section from mid-1961 to mid-1963. Although day-to-day correlation with solar activity is poor, there was a general and large decrease in  $\sigma$  during the time of decrease of solar activity as measured by sunspot number. In addition, the width of the delay spectrum and the altitude of the mean reflecting level show some correlation with sunspot number on the gross scale of these long-term averages (32).

The average values of Fig. 9 do not include measurements which indicated unusually large values of  $\sigma$ . The highest of these are shown as separate points. James (33) suggests that these measurements be treated with some

reservation because of the difficulty in handling nonthermal solar noise, but they were made in the same manner as the rest of the measurements. Additional difficulty in the early El Campo measurements arises from the fact that the echo frequency spectra were wider than the receiver bandwidth; corrections for this, based on wideband measurements obtained at a later time, have been applied to the early measurements.

The question of the possibility that the values of  $\sigma$  obtained can be unusually large also arises in connection with the Stanford measurements made in 1959, although it appears from Fig. 9 that extrapolation from even the monthly average values might give the highest individual measurement shown for this time of maximum solar activity. In the 1959 experiments the receiver bandwidth was only 2 kilohertz, while spectra taken at the shorter wavelength in 1963-64 indicate that the total echo bandwidth might have been on the order of 30 kilohertz. If a correction for this difference is applied, the two indicated points (at the top left) in Fig. 9 are obtained. A number of additional efforts have been made at Stanford since 1963, but echoes have not been reliably detected even though the radar system has been improved (34). It appears that this lack of detectable echoes may be explained in terms of the measured and extrapolated decrease of  $\sigma$  during the intervening years.

It might at first seem virtually impossible that the radar cross section for the sun could be greater by as much as two orders of magnitude than that of a smooth copper sphere the size of the photosphere, or, in other words, equal to the radar cross section of a copper sphere whose radius is 10 solar radii. It is quite clear from the measurements themselves that the reflecting regions occur usually within a few tenths of a solar radius, and certainly within one solar radius, of the photosphere (32). But radar cross section is defined in terms of a target which scatters isotropically, so that a target that preferentially scatters energy toward the receiver can have a radar cross section that greatly exceeds its physical cross section. For example, a flat reflecting region normal to the earth-sun line which has an area only one-millionth that of the solar disk would give a radar cross section at  $\lambda = 10$  meters of nearly  $10^5 \pi a^2$ . Or—to give another example—a

smooth, cylindrical, coronal streamer which is normal to the earth-sun line and of sufficient density to give total reflection would give  $\sigma \cong 20 \pi a^2$  if its radius were  $0.1 a$ , and  $n$  such streamers would yield  $\sigma \cong 20 n \pi a^2$ . It would appear possible that during periods of high solar activity the radar reflecting surface becomes more convoluted than it is during quieter periods, consisting of coronal streamers and billowing plasma of such a shape as to favor backscattering, since areas oriented to produce scattering in other directions are more likely to be shadowed behind areas oriented for reflection back to earth. Since solar activity is now increasing, we should soon have new evidence on these possible marked changes in the radar sun.

In addition to the cross-section measurements, a number of delay and frequency spectra have been obtained (32). There is a fundamental difference here, relative to the use of such spectra for planetary mapping, since, in mapping, the association with unique positions on the disk of a planet is based on the assumption of a rigid reflecting surface of near-spherical shape. For the sun, the spectra are of great interest in that they indicate large coronal motions, turbulence, variable plasma densities, a net outflow of plasma from the sun, and qualitative and quan-

titative differences both on a day-to-day basis and over the long time scale of the solar activity cycle (6, 7, 32).

If such measurements were made with a system which also gives angular resolution, the four dimensions of time delay, Doppler frequency, and two angles would provide a detailed picture of the complex, turbulent, and time-variable corona at a number of levels determined by the operating wavelengths.

### Occultation by Planets

When Mariner IV moved behind Mars after taking the historic photographs of the planet's surface, it was about  $2 \times 10^{11}$  meters from the earth. The lens-like effect of the atmosphere of Mars on the two-way radio link caused the spacecraft to appear to first move 0.75 meter closer to the earth and then to move about 2.0 meters beyond its actual path, before the signal was completely blocked by the planet. When Mariner emerged on the other side of Mars, it appeared to the radio Doppler system to be about 2.4 meters beyond its true position, but it quickly came back into proper focus without exhibiting a negative shift of the type seen during entry. Precise measurements of these small changes over this

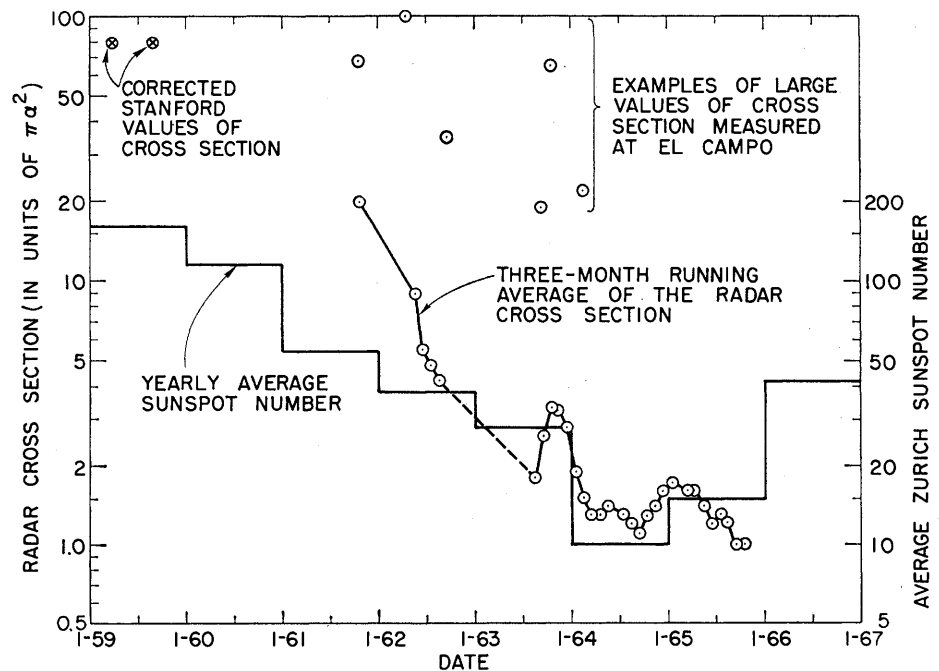


Fig. 9. Three-month running mean of the radar cross section of the sun, as measured at M.I.T.'s El Campo, Texas, field site (32), compared with the yearly average sunspot number. The radar cross sections are normalized with respect to the area of the photospheric disk. Also shown are examples of unusually large values measured at El Campo, and the 1959 results from Stanford University, including a proposed correction for echo bandwidth.

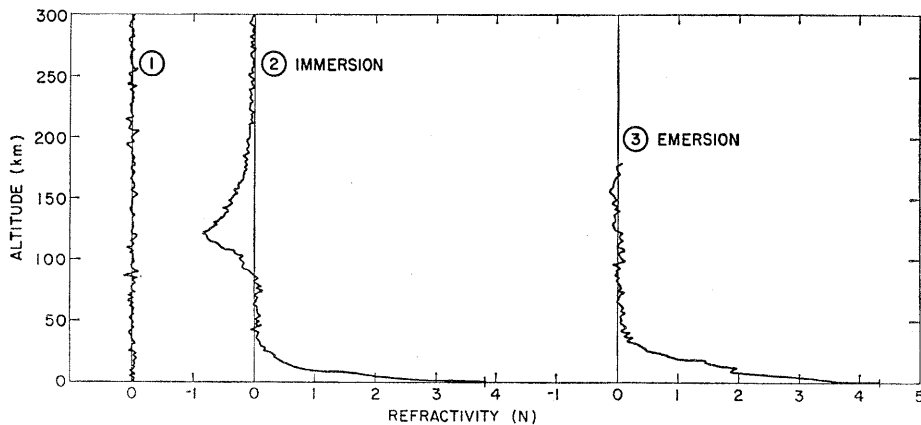


Fig. 10. Refractivity profiles for the atmosphere of Mars, derived directly from the phase measurements obtained before and after occultation of Mariner IV. Profile 1 represents the precision of the measurement when there are no atmospheric perturbations; profile 2 is based on data taken during immersion over Electris; profile 3 is based on data taken during emersion over Mare Acidalium.

vast distance provided the basic data for the radio occultation study of the neutral atmosphere and ionosphere of Mars. A number of papers have been published on the potential, planning, measurements, and interpretation of radio occultation for the study of the atmosphere of Mars (7, 35).

From the measurements of relative distance to the spacecraft, it is possible to derive a height profile of that property of the atmosphere that changes the phase velocity of the radio waves (36). Figure 10 shows profiles of refractivity  $N$  [ $N = (n - 1)10^6$ , where  $n$  is the refractive index] as a func-

tion of altitude for the atmosphere of Mars at immersion (profile 2) and emersion (profile 3). Profile 1 was produced, by means of the same method, on data obtained prior to the start of immersion, so its height scale is only relative. It serves to illustrate the fact that the departures from zero refractivity in profiles 2 and 3 represent atmospheric effects. At immersion, which occurred over a desert area (Electris) in the southern hemisphere near noon in winter, the profile shows changes in refractivity due to the lower neutral ( $N$  positive) and upper ionized ( $N$  negative) atmosphere. At emersion,

over Mare Acidalium in the Northern Hemisphere near midnight in summer, the effect of the neutral atmosphere was measured but no ionosphere was detected.

While a refractivity profile is very valuable for study of a new atmosphere, additional information is in general needed to relate the profile to the physical characteristics of the atmosphere which are of primary interest. As it turned out, however, the refractivity profiles for Mars are much more valuable than could have been anticipated, for two reasons.

First, when earth-based spectroscopic measurements of the amount of  $\text{CO}_2$  on Mars (37) are compared with the occultation measurements, it is strongly indicated that  $\text{CO}_2$  makes up the major part of the atmosphere. Thus the refractivity profiles can be interpreted with remarkably good precision in terms of pressure, temperature, mass density, and molecular number density as a function of height for the lower 30 kilometers of the atmosphere. These results are also important in theoretical analyses and extrapolations concerning surface conditions, the presence of water, the nature of the polar caps, global weather, and the evolution of the atmosphere.

Second, as seen in the immersion profile, it appears that this single-wavelength measurement has resolved both the ionosphere (where the electron number density is directly related to  $N$ ) and the lower neutral atmosphere without serious confusion. Had the ionosphere been of much lower or higher electron number density, either it might not have been detected at all (as occurred over Mare Acidalium) or else its effect might have masked the measurement of the tenuous neutral atmosphere. A two-wavelength experiment would have been more valuable in that it probably would have detected the nighttime ionosphere, provided more accurate ionospheric profiles, insured separation of all dispersive plasma effects (the earth's ionosphere, the interplanetary medium, and Mars's ionosphere) from the nondispersive effects of Mars's neutral atmosphere, and provided additional support for the view that there is no near-surface ionization to cause large errors in the deductions concerning the lower atmosphere. These considerations correspond to the earlier discussion of two-wavelength occultation measurements of the solar corona for distinguishing between the wavelength-de-

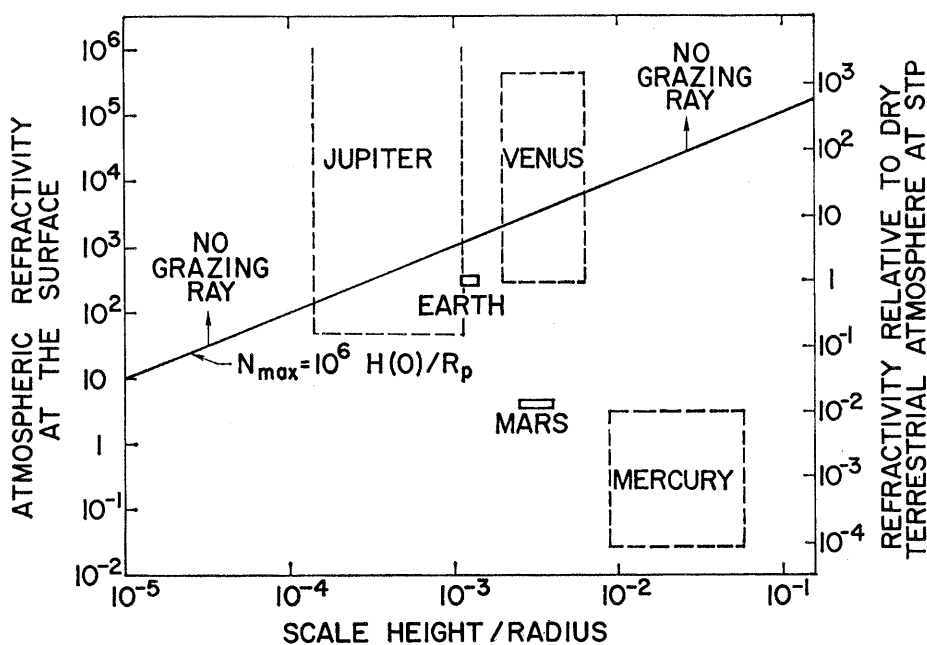


Fig. 11. Five planetary atmospheres represented in coordinates of their refractivity at the surface and the ratio of atmospheric scale height to planetary radius. If the atmospheric characteristic is above the slanting line, the radio occultation method cannot be used to probe the atmosphere all the way down to the surface, since in this region a tangential ray has a radius of curvature which is less than the planetary radius.

pendent effects of coronal electrons and the non-wavelength-dependent relativistic effects. However, as indicated above, the results for Mars appear to be such that we have relatively good profiles for the lower atmosphere under conditions where it seems unlikely that they are seriously contaminated by other effects, and important additional information is available from the ionospheric profile.

The lower-atmosphere profiles indicate a very tenuous and cold atmosphere. At immersion, the temperature was about 160°K below an altitude of 30 kilometers, and the pressure at the occultation point was about 4.5 millibars. At emersion (where the measurements are less precise), the pressure was about 8.5 millibars near the occulting surface and the temperature was about 250°K, decreasing with altitude. It would appear from the atmospheric results that the altitude of the occulting surface feature at immersion is approximately 5 kilometers greater than that at emersion, and this conclusion is supported by measurements based on the spacecraft trajectory and the time of signal loss and commencement (38). These results also suggest that the dark maria may be lower than the bright areas.

The ionospheric measurement shows a layer in which electron number density, altitude, and electron scale height are lower than had been anticipated on the basis of theory and of the limited information available prior to the flight of Mariner IV. While the measurement thus provides important limits to possible upper-atmospheric models, there remains considerable controversy on just how the profile relates to constituents, molecular number densities, temperature, and ionization production and loss mechanisms in the upper atmosphere (35). In any one model, a fairly complete picture of these characteristics follows from relatively few assumptions, but since the various models differ widely, additional study and the acquisition of new data from future missions seem to be needed to resolve the remaining problems.

At this writing a Mariner probe to Venus is due to arrive on 19 October. Radio occultation measurements will be attempted; the S-band ( $\lambda = 0.135$  meter) telemetry system will be used, as in the case of the Mariner IV occultation measurements at Mars (39). In addition, coherent transmissions from Stanford at  $\lambda = 0.71$  meter and 6.0 meters are planned. They would be received and

compared at the spacecraft, the information then being encoded and stored for later transmission to the earth as modulation on the telemetry system.

For Mars, the atmosphere was so tenuous that to detect it at all required the utmost precision of the facilities of the NASA/JPL Deep Space Net. The maximum atmospheric-induced Doppler shift was about 5 hertz. For the dense atmosphere of Venus, the maximum Doppler shift may be on the order of  $10^4$  hertz.

An important consideration here is the expectation that ray bending in the atmosphere of Venus may be so pronounced that it will not be possible to obtain refractivity profiles all the way down to the surface by the occultation technique. That is, when the radius of curvature of a tangential ray becomes as small as the radius from the center of the planet, the ray is trapped near the planet and does not reach the spacecraft. Conditions which determine whether or not this critical density is exceeded are illustrated in Fig. 11, together with known or expected characteristics of several planetary atmospheres. If the surface pressure on Venus exceeds a value of about 30 terrestrial atmospheres, there will be no surface-grazing ray received at the spacecraft. However there are still possibilities for probing beneath this critical level through use of bistatic radar reflections from the surface (40).

While one cannot predict just how important the measurements may be, there can be little doubt that precise refractivity profiles would provide more detailed information than has been available in the past for the continuing studies of Venus' atmosphere, which is expected to be fundamentally different from the atmospheres of the earth and Mars. More detailed planetary occultation measurements in the future could make use of signal amplitude, polarization, and group and phase velocity measurements for obtaining additional information on absorption, magnetic fields, temperature, and the identification and measurement of specific constituents on the basis of their absorption bands.

*Note added in proof:* The two radio occultation experiments mentioned above were among the complement of investigations successfully conducted during the Venus flyby of Mariner V on 19 October. Just the day before, the U.S.S.R. Venus 4 spacecraft detached an atmospheric landing probe which measured pressure, density, temperature,

and chemical composition of the atmosphere of Venus. The detailed information from these investigations has not yet been published. The initial reports from the Russian investigators indicate a hot (about 550°K near the surface), dense atmosphere (pressure 15 times or more that of the earth's atmosphere), almost entirely (98 percent) of CO<sub>2</sub>. As was the case for Mars, information on atmospheric constituents makes occultation measurements much more valuable, since they can then be interpreted in terms of molecular number density, pressure, and temperature as a function of height. The pressure of 15 atmospheres is less than the value given above for critical refraction. However, as my colleague G. Fjeldbo was quick to point out, the prediction was based on N<sub>2</sub> as the main constituent, and a CO<sub>2</sub> atmosphere has a smaller critical pressure because of greater refractivity and smaller scale height. On the basis of the Russian results, the atmosphere of Venus appears more than critically dense, in the sense described above. A refrigerated visitor on the surface could thus see all around the globe (the back of his head would be a distorted, multiple image on the elevated horizon), and at midnight the horizon would be uniformly bright in all directions, due to light conducted from the opposite sunlit hemisphere (it being assumed that light penetrates below the clouds). The depression he would seem to be in would follow him wherever he traveled. Trapped light near the surface might help explain the extension of the horns of the crescent of Venus and the ashen glow of the dark hemisphere—observations that have long been among the many puzzling aspects of our sister planet.

### Concluding Remarks

Radar astronomy has advanced by means of systems which were designed for, and are also used for, other purposes, such as military radar research, deep-space-probe tracking, communications research, and passive radio astronomy. Such combined use is important in increasing the effectiveness of the large investments made in these systems. However, it seems to me that the proved potential of radar astronomy studies of the solar system calls for larger facilities for this purpose and better cooperative use of equipment and installations that can do several different jobs.

As examples, I would judge the areas of greatest promise to be the following: (i) an improved monostatic, centimeter-wavelength radar system for planetary studies, in particular for radar mapping of Venus and improvements in measurements related to celestial mechanics; (ii) a greatly improved monostatic meter-wavelength radar system (operable at two or more wavelengths) primarily for solar studies, with the receiving array, which would provide good angular resolution, also used for radio astronomy studies of solar noise; and (iii) an expanded effort in bistatic radar astronomy to realize the full potential of space missions for radio science research.

In bistatic radar astronomy, the terminal on the earth could be the same as that used for monostatic radar experiments, or use could be made of the very sensitive NASA/JPL systems built for tracking deep-space probes. On the spacecraft a radio transmitter or receiver could be supplied specifically for the experiment, or use could be made of the telemetry system itself for scientific measurements. Both approaches on the earth and on the spacecraft have already been used successfully, and this will no doubt continue to be true in the future. However I believe we could do much better by taking into account the possible dual role of spacecraft and ground-based radio systems at the design stage. This is not just a one-way benefit gained by perturbing the operationally important systems in order to do more scientific experiments, since some of the proposed experiments could aid in trajectory analysis, terminal guidance, and preparation for the technological problems of future missions. Also, the added equipment could be made to provide redundant telemetry capability for higher mission reliability.

I am particularly struck by the number of interesting radio science experiments that could be conducted through use of the bistatic mode with orbiters around Mars and Venus (41). For Mars, it happens that refractivity profiles are unusually informative regarding important atmospheric and ionospheric properties, and repeated occultation measurements would reveal diurnal, seasonal, and latitudinal effects, and also the topographical relief based on the radii of the occulting features. Orbital perturbations, accurately measured by the radio links, would determine the planetary mass and moments, possible satellite effects, and (if the orbit dips

low enough) atmospheric density as well. For Venus, particular interest would center around use of the bistatic mode for obtaining high-resolution, radar-reflectivity maps of the surface, although the experiments mentioned above would of course also be of great interest. The radio links from the earth to the orbiters would show effects of the interplanetary medium and the intrusion of solar plasma streams, as in the Pioneer experiments, and would also make it possible to refine values for the planetary ephemerides and the astronomical unit. And finally, as noted above, two-wavelength links between the earth and planetary orbiters near superior conjunction may provide the ideal mode for measuring and separating radio wave perturbations due to the coronal plasma, relativistic gravitational effects on the speed of propagation of radio waves, and relativistic gravitational effects on the motion of the planets themselves.

#### References and Notes

1. "Symposium on Radar and Radiometric Observations of Venus during the 1962 Conjunction, collected papers," *Astron. J.* **69**, 1 (1964); "Symposium on Planetary Atmospheres and Surfaces, collected papers," *Radio Science* **69D**, 1617 (1965); "Proc. Caltech-JPL Lunar Planetary Conf. Sept. 1965," *JPL Tech. Mem. No. 33-266* (1966); *Solar System Radio Astronomy*, J. Aarons, Ed. (Plenum, New York, 1965); G. H. Pettengill and I. I. Shapiro, *Ann. Rev. Astron. Astrophys.* **3**, 377 (1965); J. V. Evans and T. Hagfors, *J. Geophys. Res.* **71**, 4871 (1966); D. O. Muhleman, R. Goldstein, R. Carpenter, *IEEE (Inst. Elec. Electron. Engrs.) Spectrum* **2**, 44 (1965); ———, *ibid.*, p. 78; R. M. Goldstein, *Rev. Geophys.* **2**, 579 (1964); R. B. Dyce, *Discovery* **27**, 22 (1966); G. H. Pettengill, *Intern. Sci. Technol.* **1966**, 72 (1966); ———, R. B. Dyce, D. B. Campbell, *Astron. J.* **72**, 330 (1967).
2. G. Breit and M. A. Tuve, *Phys. Rev.* **28**, 554 (1926).
3. Z. Bay, *Hung. Phys. Acta* **1**, 1 (1946); J. H. Dewitt, Jr., and E. K. Stodola, *Proc. I.R.E. (Inst. Radio Engrs.)* **37**, 229 (1949).
4. V. R. Eshleman, R. C. Barthle, P. B. Gallagher, *Science* **131**, 329 (1960); W. B. Smith, *Astron. J.* **68**, 22 (1963).
5. The paper by W. B. Smith [*Astron. J.* **68**, 22 (1963)] reports on the analysis of tape recordings made in 1959 at the Lincoln Laboratory, which show Venus echoes. Earlier reports from the Lincoln Laboratory and from Jodrell Bank, England, which seemed to show Venus echoes, now appear to represent spurious results. The tape analysis was actually made after identification of Venus echoes had been successfully made by at least four groups during the 1961 conjunction.
6. W. G. Abel, J. H. Chisholm, P. L. Fleck, J. C. James, *J. Geophys. Res.* **66**, 4303 (1961); J. H. Chisholm and J. C. James, *Astrophys. J.* **140**, 377 (1964); W. K. Victor and R. Stevens, *Science* **134**, 46 (1961); Staff, M.I.T. Lincoln Laboratory, *Nature* **190**, 592 (1961); I. Maron, G. Luchak, W. Blitzstein, *Science* **134**, 1419 (1961); J. H. Thomson, J. E. B. Ponsoby, G. N. Taylor, R. S. Roger, *Nature* **190**, 519 (1961); V. A. Kotelnikov and L. V. Apraksin, *Radiotekhn. i Elektron.* **7**, 1851 (1962).
7. V. R. Eshleman, in *Solar System Radio Astronomy*, J. Aarons, Ed. (Plenum, New York, 1965); J. C. James and R. P. Ingalls, *Astron. J.* **69**, 19 (1964).
8. M. Ash, I. I. Shapiro, W. B. Smith, *Astron. J.* **72**, 338 (1967).
9. I. I. Shapiro, *Phys. Rev. Letters* **13**, 789 (1964); D. O. Muhleman and P. Reichley, in *JPL Space Programs Summary No. 37-29* (1964), vol. 4, p. 239; D. K. Ross and L. I. Schiff, *Phys. Rev.* **141**, 1215 (1966).
10. D. W. Trask et al., "Physical Constants as Determined from Radio Tracking of the Ranger Lunar Probes," *JPL Document TR-32-1057* (1966); J. D. Anderson, "Determination of the Masses of the Moon and Venus and the Astronomical Unit from Radio Tracking Data of the Mariner IV Spacecraft," *JPL Document TR-32-816* (1967).
11. H. T. Howard, V. R. Eshleman, G. H. Barry, R. B. Fenwick, *J. Geophys. Res.* **70**, 4357 (1965); H. T. Howard, *ibid.* **72**, 2729 (1967); P. Yoh, H. T. Howard, B. B. Lusignan, V. R. Eshleman, *ibid.* **71**, 189 (1966).
12. Staff, Stanford Center for Radar Astronomy, *J. Geophys. Res.* **71**, 3325 (1966); H. T. Howard and R. L. Koehler, in "Proceedings of the Conference on Zodiacal Light and the Interplanetary Medium, Honolulu, 1967," in press; R. L. Koehler, "Interplanetary Electron Content Measured between Earth and the Pioneer VI and VII Spacecraft Using Radio Propagation Effects," *Stanford Univ. Rep. No. SEL 67-051* (1967).
13. A. Hewish, P. A. Dennison, D. H. Pilkington, *Nature* **209**, 1188 (1966); O. B. Slee, *Planetary Space Sci.* **14**, 255 (1966); M. H. Cohen, *Nature* **208**, 277 (1965); E. E. Salpeter, *Astrophys. J.* **147**, 433 (1967); M. H. Cohen, E. J. Gunderman, H. E. Hardebeck, L. E. Sharp, *ibid.* **147**, 449 (1967).
14. R. M. Goldstein et al., "The Superior Conjunction of Mariner IV," *JPL Tech. Rep. No. 32-1092* (1967).
15. G. H. Pettengill, in *Solar System Astronomy*, J. Aarons, Ed. (Plenum, New York, 1965); J. V. Evans and G. H. Pettengill, in *The Moon, Meteorites and Comets*, B. M. Middlehurst and G. P. Kuiper, Eds. (Univ. of Chicago Press, Chicago, 1963).
16. T. Hagfors, R. A. Brockelman, H. H. Danforth, L. B. Hanson, G. M. Hyde, *Science* **150**, 1153 (1965).
17. G. H. Pettengill and J. C. Henry, *J. Geophys. Res.* **67**, 4881 (1962).
18. R. M. Goldstein, *Science* **144**, 842 (1964); V. A. Kotelnikov and B. M. Du Brovin, *Dokl. Akad. Nauk. SSSR* **155**, 1037 (1964).
19. J. V. Evans, R. P. Ingalls, L. P. Rainville, R. R. Silva, *Astron. J.* **71**, 902 (1966).
20. R. L. Carpenter, *ibid.* **69**, 2 (1964); R. M. Goldstein, *ibid.*, p. 12.
21. G. H. Pettengill, H. W. Briscoe, J. V. Evans, E. Gehrels, G. M. Hyde, L. G. Kraft, R. Price, W. B. Smith, *ibid.* **67**, 181 (1962); D. O. Muhleman, D. B. Holdridge, N. Block, *ibid.*, p. 191.
22. D. Muhleman, *ibid.* **66**, 292 (1961); J. E. B. Ponsoby, J. H. Thomson, K. S. Imrie, *Nature* **204**, 63 (1964); R. L. Carpenter, *Astron. J.* **69**, 2 (1964); W. K. Klemperer, G. R. Ochs, K. L. Bowles, *ibid.*, p. 2; R. M. Goldstein, *ibid.*, p. 12; V. A. Kotelnikov, *Radio Sci.* **69D**, 1634 (1965); R. M. Goldstein, *ibid.*, p. 1623; I. I. Shapiro, *ibid.*, p. 1632; R. B. Dyce, in "Proceedings of The Caltech-JPL Lunar and Planetary Conference, 1965," *JPL Tech. Mem. No. 33-266* (1966), p. 172; R. M. Goldstein, paper presented at The International Space Science Symposium COSPAR, 7th, Vienna, Austria, May 1966.
- 22a. Note added in proof: A newer value based on measurements is  $-243.9 \pm 0.18$  days [I. I. Shapiro, *Science* **157**, 423 (1967)].
23. P. Goldreich and J. H. Peale, *Nature* **209**, 1117 (1966).
24. G. H. Pettengill, in "15th General Assembly International Scientific Radio Union," *Nat. Acad. Sci.-Nat. Res. Council Pub.* **1468** (1966); R. B. Dyce, G. H. Pettengill, I. I. Shapiro, *Astron. J.* **72**, 351 (1967).
25. I. Velikovsky, *Worlds in Collision* (Dell, New York, 1965).
26. R. L. Carpenter and R. M. Goldstein, *Science* **142**, 381 (1963).
27. G. H. Pettengill and R. B. Dyce, *Nature* **206**, 1240 (1965).
28. W. E. McGovern, S. H. Gross, S. I. Rasool, *ibid.* **208**, 375 (1965); H. S. Liu and J. A. O'Keefe, *Science* **150**, 1717 (1965).
29. G. H. Pettengill, private communication.
30. G. L. Tyler, V. R. Eshleman, G. Fjeldbo, H. T. Howard, A. M. Peterson, *Science* **157**, 193 (1967); G. L. Tyler, *J. Geophys. Res.* **71**, 1559 (1966).
31. L. F. Dellwig and R. K. Moore, *J. Geophys. Res.* **71**, 3597 (1966); L. J. Cutrona, W. E. Vivian, E. N. Leith, G. O. Hall, *I.R.E. (Inst.*

- Radio Engrs.) Trans. Military Electron.* 5, 127 (1961).
32. J. C. James, *Astrophys. J.* 146, 356 (1966).
33. ———, private communication.
34. J. E. Ohlson, thesis, Stanford University, 1967.
35. "A Review of Space Research," *Nat. Acad. Sci.-Nat. Res. Council Pub.* 1079 (1962), chap. 6; G. Fjeldbo and V. R. Eshleman, *J. Geophys. Res.* 70, 13 (1965); G. Fjeldbo, V. R. Eshleman, O. K. Garriott, F. L. Smith, III, *ibid.*, p. 3701; A. J. Kliore, D. L. Cain, G. S. Levy, V. R. Eshleman, F. D. Drake, G. Fjeldbo, *Astronaut. Aeronaut.* 7, 72 (1965); A. Kliore, D. L. Cain, G. S. Levy, V. R. Eshleman, G. Fjeldbo, F. D. Drake, *Science* 149, 1243 (1965); F. S. Johnson, *ibid.* 150, 1445 (1965); S. H. Gross, W. E. McGovern, S. I. Rasool, *ibid.* 151, 1216 (1966); J. W. Chamberlain and M. B. McElroy, *ibid.* 152, 21 (1966); T. M. Donahue, *ibid.*, p. 763; G. Fjeldbo, W. C. Fjeldbo, V. R. Eshleman, *J. Geophys. Res.* 71, 2307 (1966); ———, *Science* 153, 1518 (1966); "Proceedings Conference on Atmospheres of Mars and Venus, Tucson, 1967," in press.
36. G. Fjeldbo, "Bistatic Radar for Studying Planetary Ionospheres and Surfaces," *Stanford Univ. Rep. No. SEL 64-025* (1964).
37. L. D. Kaplan, G. Munch, H. Spinrad, *Astrophys. J.* 139, 1 (1964); M. J. S. Belton and D. M. Hunten, *ibid.* 145, 454 (1966).
38. A. J. Kliore, D. L. Cain, G. S. Levy, paper presented before the 7th International Space Science Symposium, COSPAR, Vienna, 1966.
39. A. Kliore, D. A. Tito, D. L. Cain, paper presented before the 5th Aerospace Sciences Meeting, New York, January 1967.
40. G. Fjeldbo, paper presented before the 5th Aerospace Sciences Meeting, New York, January 1967.
41. V. R. Eshleman, *Astronaut. Aeronaut.* 5, 16 (1967).
42. I thank NASA for financial support of the radar astronomy research at the Stanford Center for Radar Astronomy (a joint research group with Stanford Research Institute) and my colleagues of the Center for help in preparing this review article—in particular, R. B. Dyce, G. Fjeldbo, H. T. Howard, R. L. Koehler, L. A. Manning, and G. L. Tyler. I also thank G. H. Pettengill and J. C. James of the Lincoln Laboratory and M.I.T. for their assistance.

## Ecological Ectocrines in Experimental Epidemiology

A new class, the "pacifarins," is delineated in the nutritional ecology of mouse salmonellosis.

Howard A. Schneider

The general subject of the nutrition of hosts as a factor in resistance to infectious disease has hardly languished for want of discussion (see 1, 2). But I think it may be fairly asked whether the accomplishments in this area are comparable to those of modern scientific nutrition in some other areas of public health. The reason for my skepticism is this: If nutrition is to be viewed as being effective, either theoretically or practically, as a means of coping with infectious disease, then it inevitably must be judged in the light of other theoretically fruitful and demonstrably successful measures, such as sanitation, vaccination, and antibiotics. In this comparison, it must be admitted, nutrition suffers.

But if, in this context, nutrition is relatively downgraded both by the theoretician and by the decision maker in the field of public health, why is there a periodic resurgence of interest in, and discussion of, nutrition and infection? This perennial florescence of interest and discussion follows, I think, from several considerations, some of them not strictly scientific. To ignore them, however, would be unscientific.

Apologists for nutrition as a factor in resisting disease draw attention, for example, to the historical connection between famine and pestilence. This association, however, may be a matter more of concomitance than of causality. Results of modern scientific studies of nutrition in animals suggest that in nutritional science we may have an instrumentality not yet used widely enough or discerningly enough for our ends. These new studies raise newer hopes. Again, modern nutritional science has led to the control of certain well-defined diseases, such as scurvy, beriberi, pellagra, rickets, and some of the anemias. The continuing hope of similarly and nutritionally controlling other diseases, such as coronary thrombosis, hypertension, allergic states, and mental abnormalities, spurs investigators to wrestle once again with an old problem.

With this cursory synopsis of the contemporary mood and the past history of the problem, an explanation for any attempt to inject fresh meaning into the subject would seem in order. My explanation is this. Through circumstance I have been able to sus-

tain investigation of the problem of nutrition and infectious disease for a relatively long time (3), and certain features and results of the investigation to date move me to take a new and hopeful view. After long years of doubting, I now assert (i) that a specifiable relationship does exist between host nutrition and response to infectious disease; (ii) that I have reached this conclusion through animal experiments based on a new and unique experimental design; (iii) that this design follows from an analysis of the problem in ecological concepts that go beyond classical concepts in the fields of nutrition and microbiology; (iv) that, in the case of mouse salmonellosis (an infectious disease model), an organic compound representing a new class of compounds has been discovered in the nutritional environment, which, when ingested in very small amounts, greatly increases the host's chance of survival; and (v) that this new compound has features similar to those of ecological ectocrines.

### Historical Origins

#### of the New Approach

Investigations into infectious disease classically have their origins in the field. The investigation discussed here originated, not in field studies, but in what was once known as "experimental epidemiology"—that is, the study in the laboratory of a "natural" infectious disease in populations of experimental animals. The notion of experimental epidemiology clearly can be traced to a proposal by Topley in his Goulstonian lecture of 1919 (4). What Topley proposed was not the use of the lab-

The author, formerly at the Rockefeller Institute, is now a member of the Institute for Biomedical Research, Education and Research Foundation, American Medical Association, Chicago, Illinois.